A finite-difference time-domain investigation of reflections from layered wall structures

Aki Haapaniemi (aki.haapaniemi@aalto.fi)
Alex Southern (mrapsouthern@gmail.com)
Tapio Lokki (tapio.lokki@aalto.fi)
Department of Media Technology
Aalto University School of Science
P.O. Box 15500, FI-00067 Aalto, Finland

ABSTRACT

The acoustic reflection characteristics of layered wall structures were studied using the 2-D standard rectilinear (SRL) finite-difference time-domain (FDTD) method. The studied structures feature a slatted panel combined with a back wall, forming a cavity in between. The visual appearance of such structures resembles slatted resonant absorbers, but in this case the slat width is considerably wider and no absorptive material is present behind the panel. The types of structures studied here are found in use in some concert halls, e.g. in the Helsinki Music Centre concert hall in Finland. In the simulations, the structural features were varied in order to see how the reflection characteristics change with the features. The reflection responses are presented by normalizing the average frequency response of a line of multiple receiver points with respect to the corresponding average for a flat wall. Additional simulations were done to study the diffusive properties of such structures. Furthermore, 2-D FDTD visualizations of reflections from the structures are included to facilitate intuitive understanding. The structures were found to exhibit various degrees of comb filtering effects and frequency-dependent spatial and temporal spreading.

1   INTRODUCTION

Modern vineyard type concert halls often have surfaces that are close to seats. Therefore, there might be a need to design such surfaces so that they do not give out strong reflections that could dominate the sound at those seats. For example, Figures 1a and 1b show one such wall directly behind a seating area at the Helsinki Music Centre Concert Hall during construction. Figure 1a shows the back wall structure, a sawtooth-shaped corrugated wall made out of concrete. In front of the wall are metal supports, on which wooden slatted panels will later be installed. Figure 1b shows one such panel, waiting for installation. The panels are installed so that the slats are horizontal, and the complete structures are situated behind seating areas, e.g. as shown in Figure 1c.

However, it is not trivial to predict how sound reflects from such a layered wall structure. This paper shows the results of a study in which reflection of sound from two types of slatted panel structures with different back wall shapes were simulated with a wave-based modelling technique:
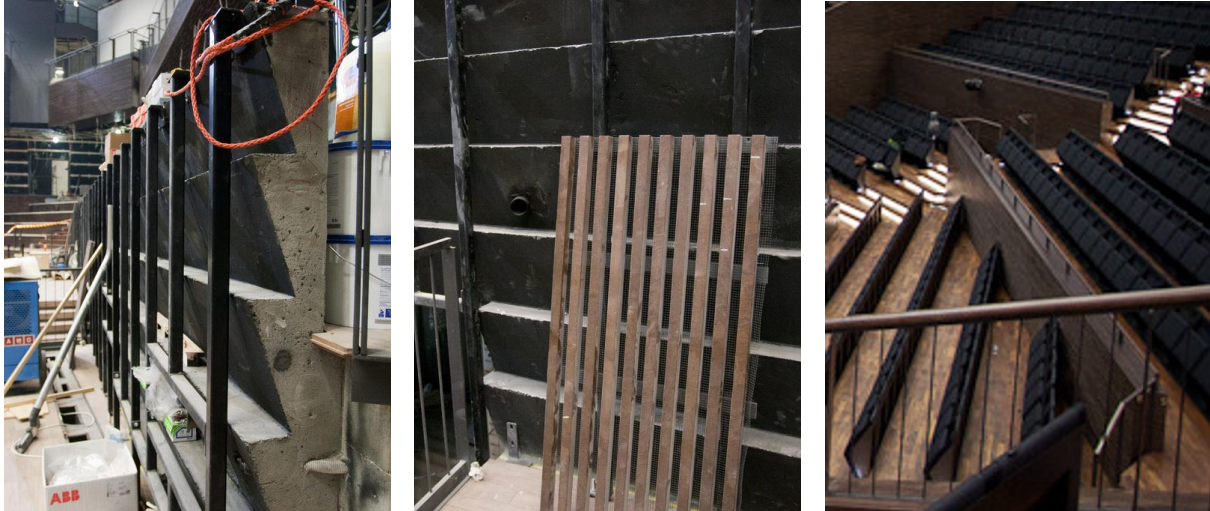
(a) Corrugated back wall.   **(b)** Slatted panel.   **(c)** Complete structures.

Figure 1: Audience area back walls at the Helsinki Music Centre Concert Hall. Photos courtesy of Jukka Pätynen.

the 2-D standard rectilinear (SRL) finite-difference time-domain (FDTD) method[1]. The results are presented from three points of view: visualizations facilitate intuition, frequency-domain analysis allows detailed examination, and diffusive properties are examined with polar response measurements and corresponding diffusion coefficients.

2 STUDIED WALL STRUCTURES

A 2-D vertical cross-section model was made based on the photos in Figure 1. A 5 cm $\times$ 5 cm slatted panel with 50 % open area was combined with a sawtooth-shaped back wall corrugation of period length 40 cm. The amplitude of the corrugations was chosen as 15 cm, thus resulting in minimum and maximum cavity depths of 5 cm and 20 cm, respectively. The width of the whole structure was made larger than what is seen in the photo: the width was set as 4.25 m for the frequency domain investigation and visualizations. For the polar response simulations, the model width was chosen smaller (2.1 m) because of constraints set by the measurement method and the associated high computational demands.

An otherwise similar model was made with a flat wall in place of the corrugated wall. In this paper, the effect of these two types of structures are gauged by means of comparisons. Henceforth the two structure types will be referred to as *structure A* (slatted panel/flat back wall) and *structure B* (slatted panel/saw corrugated back wall). Models with different overall cavity depths, corrugation depths and corrugation periods were also made but their effects will be only briefly reported because of limited space. Apart from the differences in the full model widths (i.e. 4.25 m and 2.1 m), the slatted panel is kept similar in all the models studied in this paper. The reader is referred to a more thorough investigation[2] for the details concerning various structural parameters.

3 VISUALIZATIONS

For the visualization simulations a sampling frequency of 200 kHz was used in order to maximize visual quality. The source type used is a *transparent source*[3], i.e. a source that does not scatter

incident energy (as opposed to a *hard source*), situated at a boundary node 5 meters from the slatted panel. All the later simulations presented in this paper also use transparent sources. A low pass impulse with a cutoff frequency at 10 kHz was used as the source signal to avoid visual aliasing. The reflection coefficient was 0.95 for all surfaces except at the transition point from the studied structure to the simulation space boundary, which was made absorptive by applying to it a reflection coefficient value of 0.001. Screenshots were taken of the two simulations and combined to form the series of images shown in Figure 2.
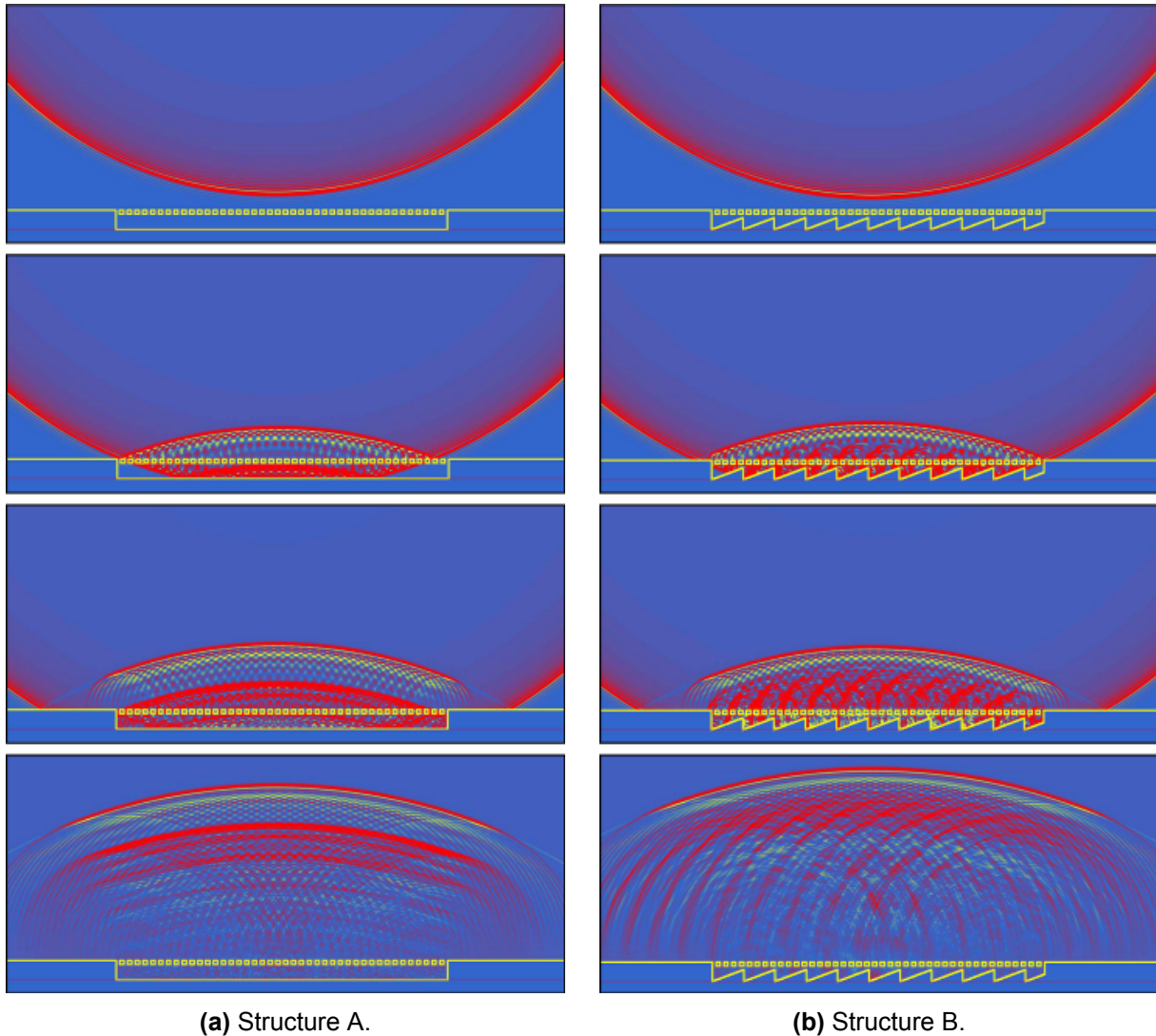

(a) Structure A.   (b) Structure B.
Figure 2: 2-D FDTD visualizations of reflections from two layered wall structures.

For *structure A*, Figure 2a shows the following effects. The incident wave is partly reflected by, and partly transmitted through the slatted panel. The transmitted wave is then reflected back from the cavity wall, and part of the wave passes through the panel while part of it is reflected back towards the cavity wall. In this manner, the total outgoing wave is a series of consecutive wavefronts, delayed according to the depth of the cavity and filtered by the panel. For *structure B* (Figure 2b), the effect of the cavity wall corrugation can be seen in that the delayed wavefronts are broken up into multiple smaller wavefronts that distribute some of the energy to the side directions.

3

The diffusive effect of the back wall corrugation is therefore clearly observed in the visualizations. Furthermore, the wavefronts directed to the left of the structure are slightly more pronounced due to the orientation of the corrugation.

4 FREQUENCY DOMAIN STUDIES

While the visualizations are informative, they do not reveal what occurs at different frequencies. Therefore, another set of simulations were performed to study the frequency content of the reflections. For these simulations a sampling frequency of 48.6 kHz was used. It ensures true enough representation of the structures (internodal distance is approximately 1 cm) and a sufficiently broad valid frequency range in terms of dispersion, whilst keeping the computing demands at a feasible level. The reflection coefficient was set similarly as in the visualization simulations. A receiver arrangement of six lines of 20 receiver points was used, as shown on the left image in Figure 3. The first line is at a distance of 1.25 m from the panel surface and each consecutive line is 1 m further away. The distance between adjacent receiver points in a line is 10 cm. The source (not shown in the image) was positioned at a boundary node 15 m away from the panel surface, on the same horizontal position as the leftmost receivers of each line.
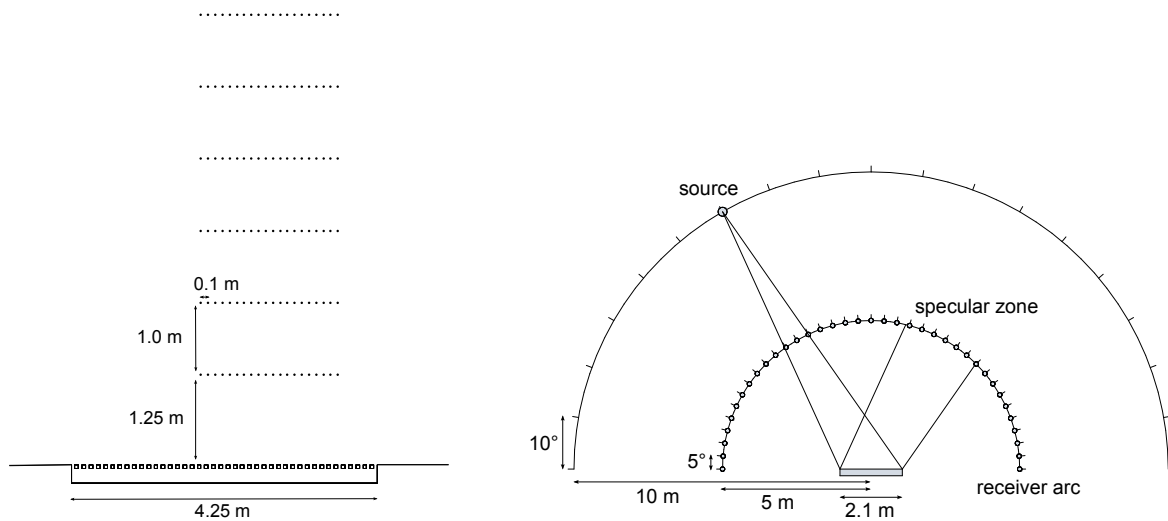

Figure 3: The arrangements for the frequency domain (left) and polar response (right) studies.

In order to exclude the effect of the direct sound, a subtraction technique[4] was used. The direct sound was separately simulated for the same source/receiver arrangement in an essentially empty space, and subtracted from the results of the reflection simulations. The analyzed results therefore consist of only the reflection at each receiver point. The results were also low-pass filtered and windowed with a tapered window (a vector of ones concatenated with a half Hann-window) to prevent aliasing and truncation artifacts from contaminating the results. FFT's were computed for the windowed results, after which the frequency responses were averaged by lines of receivers to obtain the mean frequency responses for each line. Averaging the results over multiple receiver points helps in emphasizing the prominent effects by averaging out the more chaotic variations.

In 2-D FDTD, the *afterglow*[5] effect must also be taken into account. It manifests as an asymptotic impulse in the time domain and a low frequency emphasis in the transfer domain. A suitable compensation has been derived for free-space propagation[5], but a compensation scheme for a more practical situation is yet to be conceived. Here the afterglow effect is compensated for by

normalizing the mean frequency responses for lines of receivers with the corresponding results for a flat wall.
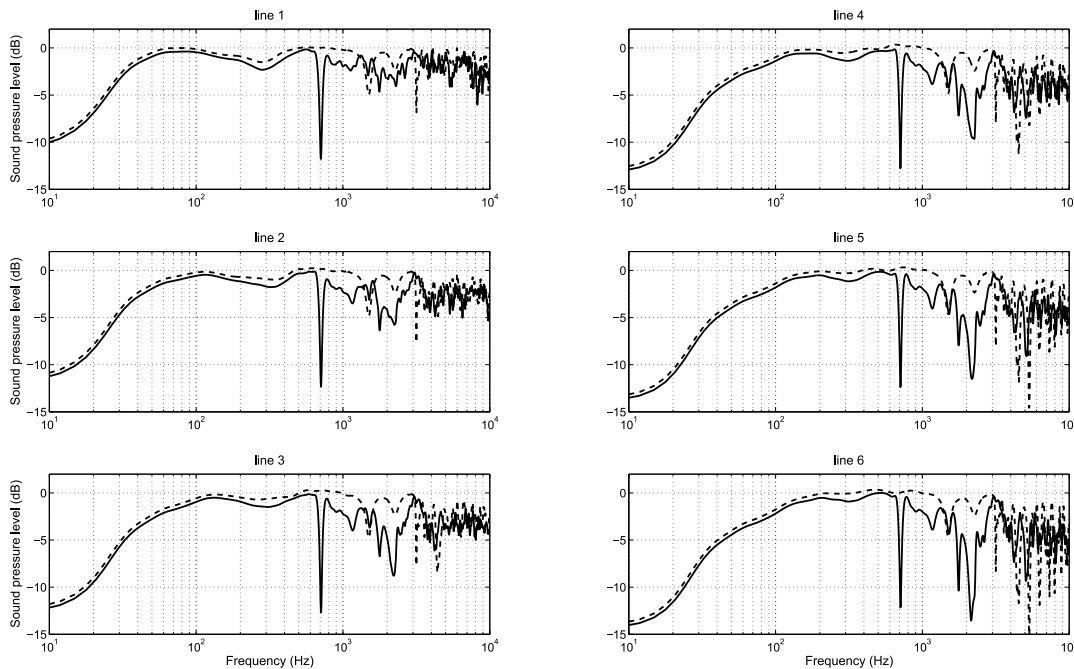

Figure 4: Mean frequency responses for six lines of receivers for structure A (dashed line) and structure B (solid line) with the same average cavity depth.

The results for structures A and B are shown in Figure 4. The cavity depth of *structure A* is 12.5 cm in order to give equal average depth as *structure B*. The overall shapes of the mean frequency responses for both structures are similar from low frequencies up to about 600 Hz. The responses from both structures also have a well-matched notch at approximately 1.5 kHz, which is therefore due to the panel or the size of the cavity (rather than the shape). However, for *structure B* a very narrow notch that exceeds 10 dB in depth is found at 700 Hz for all lines of receivers. In addition, some high frequency loss is evident between 700 Hz and 3 kHz, the greatest notch being at slightly above 2 kHz. The effect becomes more prominent with increasing distance, which suggests diffusive behaviour. The exact reason for the apparent low frequency loss below 100 Hz is not known, but it is probably related to the width of the studied structures.

As the visualization in Figure 2 shows, *structure A* has an effect of spreading the incident wave in time by filtering (panel) and delaying (cavity). This effect is further analyzed in Figure 5 with mean frequency responses and spectrograms of the reflections for models of different cavity depths. The time-domain response up to about 3 ms (Figure 5, on the right) is common to all cavity depths and is due to the panel[2]. With 20 cm cavity depth the first back wall reflection overlaps with the panel response. The later part of the responses is affected by the cavity depth. In the mean frequency responses (Figure 5, on the left) this is seen as a comb filtering effect. However, although the notch frequencies are found at roughly harmonic multiples and are dependent on the cavity depth, the frequencies are not predicted by either 1/2 or 1/4 wavelength resonances. Further studies[2] show that the first notch in the mean frequency responses of *structure B* also depend on the overall cavity depth but in a different and less predictable way. Moreover, both corrugation period length and amplitude of the corrugations show an effect on the first notch: larger features lower the frequency.
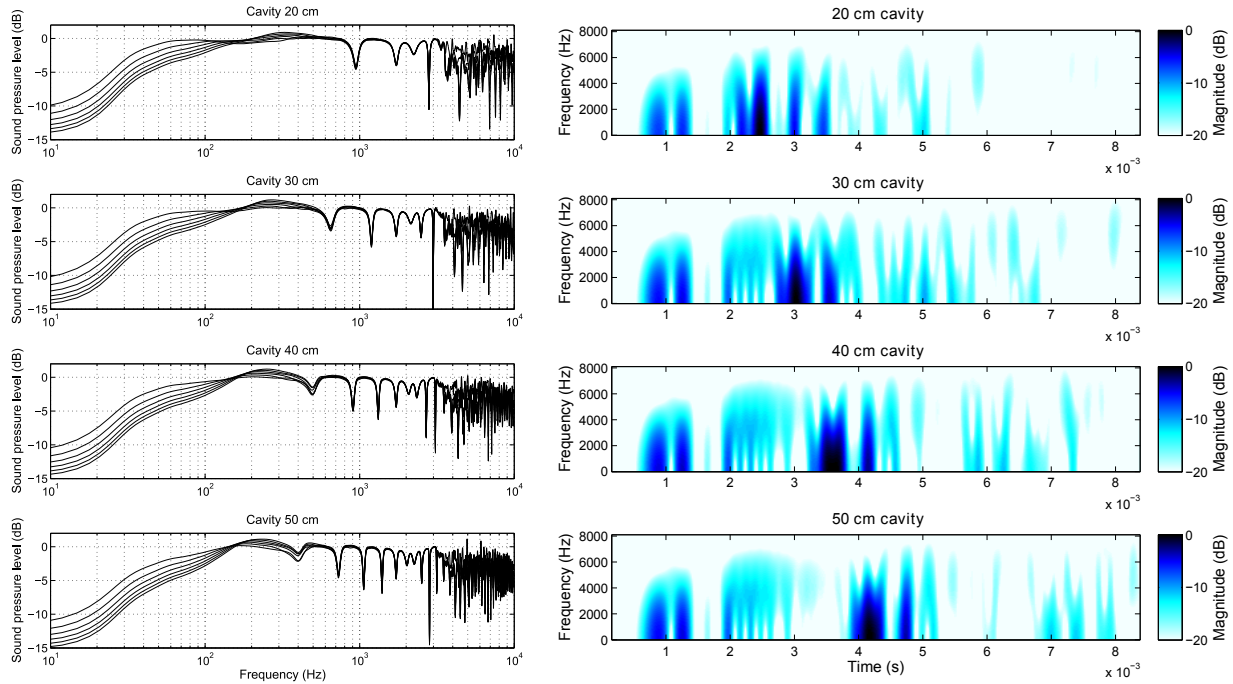
Figure 5: The effect of the cavity depth of *structure A* on the mean frequency responses for six lines of receivers (left) and the time domain response of a single receiver at the middle of the 6th line of receivers (right).

5   POLAR RESPONSE STUDIES

The diffusive properties of the two structure types were studied with the standard technique for polar response measurements[6,7]. The sampling frequency was 48.6 kHz. The measurement arrangement is shown in Figure 3 on the right. 37 receiver points were positioned on a semicircle, $5°$ apart and at a radius of 5 meters from the center of the target structure. 19 source positions were likewise positioned on a semicircle, $10°$ apart and at a radius of 10 meters from the center of the structure. A reflection coefficient of 0.95 was assigned to the structures.

The width of the sample structure was 2.1 meters. It is quite large compared to the measurement setup geometry, but still conforms to the standard recommendation of having at least 80 % of the receivers outside the specular zone for each source position. For periodic structures, the sample structure should have at least four full periods in order for the results to be representative of the full structure[7]. The width used here accommodates five full periods of the 40 cm length corrugations, including the enclosing edges. Structures A and B are similar to those studied in Section 4, except for their width and thus the number of corrugation periods and slats. The difference is unavoidable due to limitations imposed by the requirements of the polar response measurement method. The wider structure would require too big a mesh for simulation with the available resources.

In accordance to the measurement technique specifications, the simulations were also run for a reference flat panel of equal dimensions, for reference purposes and diffusion coefficient normalization. The normalization is done to eliminate the edge diffraction effects that lead to overestimation of diffusion coefficient values at low frequencies. Additionally, the simulations were run in an essentially empty space in order to obtain the direct sound at receivers, for subtraction purposes.

The results were filtered to get rid of aliasing effects and the direct sound was subtracted from the sample structure and reference panel responses. The start points for the individual reflection responses were algorithmically detected for automatic and accurate placement of windows. A tapered window was applied to avoid truncation problems.
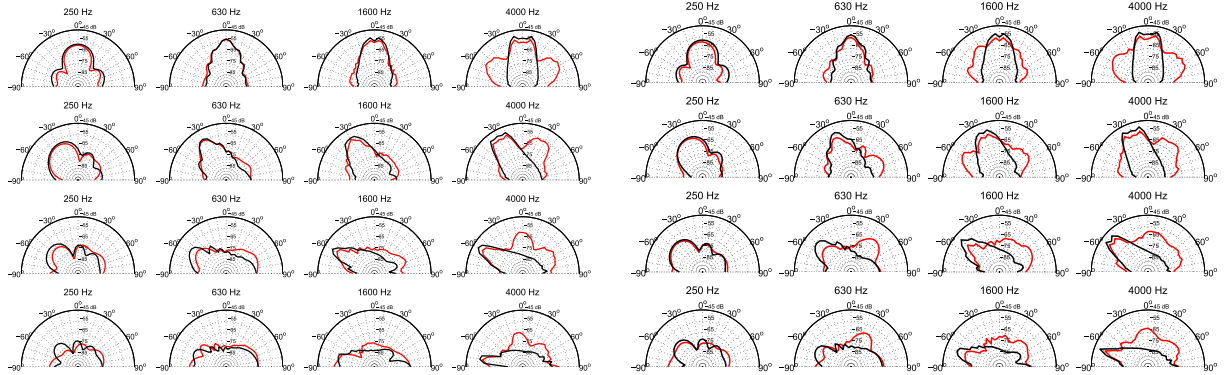

Figure 6: Polar responses for a subset of 1/3 octave bands for $0°$ (first row), $20°$ (second row), $50°$ (third row) and $70°$ (bottom row) incidence angles; black lines = reference flat panel, red lines = structure A (left) / structure B (right).

After isolating and windowing the responses, the energy of each individual receiver response was summed up over 1/3 octave bands and the 37 responses for one source position were combined to form the polar response for a specific angle of incidence. This procedure was done for all angles of incidence. Figure 6 shows a subset of the polar responses for both of the structures along with the reference responses. For *structure B*, there is no diffusion in the 250 Hz band but in the 630 Hz band a diffusing effect is already evident, especially at oblique angles. This effect is likely due to the corrugated back wall because it is in this frequency range that the back wall corrugation dimensions are comparable to the wavelength. The higher frequency bands show more diffusion for both structures and also at normal incidence, which suggests that the panel plays a significant role in the diffusion at these frequencies. Compared to *structure B*, *structure A* is clearly less diffusive at the 630 Hz and 1600 Hz bands, while in the 4 kHz band the amount of diffusion is prominent, although still less than for *structure B*.

The next step was to quantify the amount of diffusion in different frequency ranges by calculating the diffusion coefficients. The autocorrelation diffusion coefficient values for the 1/3 octave bands for each angle of incidence were calculated with[7]

$$d_\theta = \frac{(\sum_{i=1}^{n} 10^{L_i/10})^2 - \sum_{i=1}^{n}(10^{L_i/10})^2}{(n-1)\sum_{i=1}^{n}(10^{L_i/10})^2} \ , \tag{1}$$

where L_i are sound pressure levels (in dB), n is the number of receivers and θ is the angle of incidence. The final diffusion coefficient value is obtained by averaging the diffusion coefficient values over all angles of incidence. The normalized diffusion coefficient is then calculated by subtracting the values obtained for the flat panel from the diffusion coefficient[7]:

$$d_{\theta,n} = \frac{d_\theta - d_{\theta,r}}{1 - d_{\theta,r}} \ . \tag{2}$$

7

Here $d_{\theta,r}$ is the diffusion coefficient value for the reference panel. In case the normalization results in negative diffusion coefficient values for some 1/3 octave bands, these values are manually rectified to 0. The diffusion coefficient values for the reference panel as well as both the unnormalized and normalized diffusion coefficient values for structures A and B are shown in Figure 7.
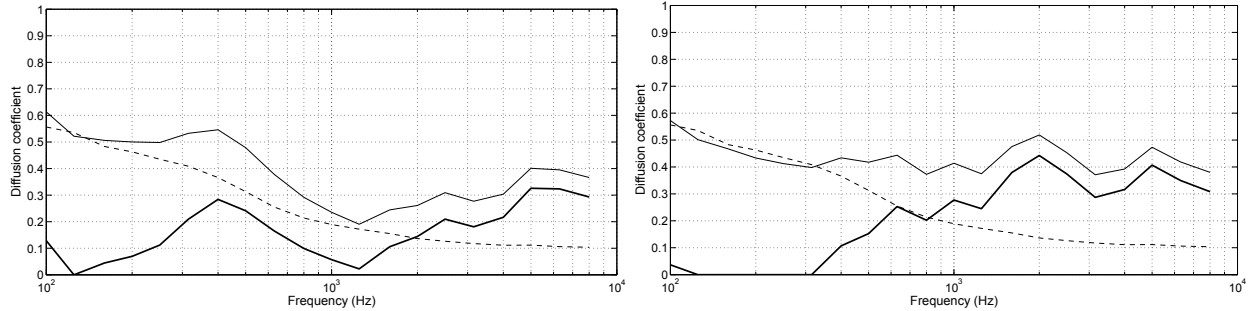

Figure 7: The diffusion coefficient values for structures A (solid line, left) and B (solid line, right). The dashed line shows the diffusion coefficient values for the reference flat panel and the thick lines denote the normalized diffusion coefficient values.

The maximum of the diffusion coefficient for *structure B* is found at 2 kHz, which corresponds to the notch found in the mean frequency responses in Figure 4. The notch is more prominent for further receiver distances because the structure is particularly diffusive at these frequencies. The sound energy still registers in the responses of receiver lines near the structure – because the redirected path is within their reach – but evades the more distant receiver lines.

Comparison of the diffusion coefficients shows that *structure B* is considerably more diffusive between about 600 Hz and 5 kHz. However, *structure A* shows more diffusion at and below about 500 Hz. It is below these frequencies that the wavelength becomes comparable to the cavity width (2 m). Therefore it may be a source of resonances at this frequency range, especially for high incidence angles. It may be due to these resonances being less inhibited because of the flat back wall that *structure A* has a higher diffusion coefficient value compared to *structure B*.

6 SUMMARY

The sound reflection properties of two types of layered wall structures were studied with 2-D SRL FDTD simulations using visualizations, frequency-domain analysis and polar response measurements. The studied structures consist of a slatted panel coupled with a back wall, forming a cavity in between. Two structure types with different back wall shapes were studied: flat (*structure A*) and periodic saw corrugation (*structure B*). *Structure A* created a resonant system where the panel acts as a filter, and the cavity acts as a delay line. The overall reflected sound was seen to consist of multiple successive wavefronts, generated by the combination of delays imposed by the cavity depth, and the filtering by multiple interactions with the panel. In the time domain, the effect was seen as the spreading of the incident sound, the extent of which was dependent on the cavity depth. In the frequency domain, a comb filter effect was seen.

For *structure B*, the mean frequency responses show a very narrow and deep notch at 700 Hz. The frequency of this notch was influenced by the overall cavity depth, the length of the corrugation period and the amplitude of the corrugation. Furthermore, *structure B* was found to have diffusive/attenuative properties at frequencies above about 500 Hz. The polar response studies revealed a maximum value for the normalized diffusion coefficient of almost 0.45 at the 1/3 octave

8

band centered on 2 kHz. This maximum value coincides with the mean frequency responses that show a clearly identifiable notch at the same frequency range for the further lines of receivers. This shows that the notch results from the diffusive properties of the structure. On the other hand, *structure A* does not exhibit appreciable diffusion at the same frequency range. Therefore the saw corrugated back wall can be said to be the influence behind majority of the diffusion in the mid to high frequency range for *structure B*.

ACKNOWLEDGMENTS

REFERENCES

1 S. Bilbao. *Wave and scattering methods for numerical simulation*. Wiley, first edition, 2004.
2 A. Haapaniemi. Simulation of acoustic wall reflections using the finite-difference time-domain method. Master's thesis, Aalto University School of Electrical Engineering, 2012.
3 J. Schneider. Implementation of transparent sources embedded in acoustic finite-difference time-domain grids. *J. Acoust. Soc. Am.*, 103:136–142, 1998.
4 E. Mommertz. Angle-dependent in-situ measurements of reflection coefficients using a subtraction technique. *Applied Acoustics*, 46:251–263, 1995.
5 C. Spa, J. Escolano, A. Garriga, and T. Mateos. Compensation of the afterglow phenomenon in 2-D discrete-time simulations. *IEEE Signal Processing Letters*, 17:758–761, 2010.
6 AES-4id-2001. AES information document for room acoustics and sound reinforcement systems – characterization and measurement of surface scattering uniformity. *J. Audio Eng. Soc.*, 49:149–165, 2001.
7 T. J. Cox and P. D'Antonio. *Acoustic Absorbers and Diffusers: Theory, design and application*. Taylor & Francis, second edition, 2009.